1-1-2015

Aspirin inhibits formation of cholesterol rafts in fluid lipid membranes

Richard J. Alsop
McMaster University

Laura Toppozini
McMaster University

Drew Marquardt
Brock University

Norbert Kučerka
National Research Council Canada

Thad A. Harroun
Brock University

See next page for additional authors

Biochimica et Biophysica Acta 1848 (2015) 805–812

Contents lists available at ScienceDirect

Biochimica et Biophysica Acta

journal homepage: www.elsevier.com/locate/bbamem

Aspirin inhibits formation of cholesterol rafts in fluid lipid membranes

Richard J. Alsop [a], Laura Toppozini [a], Drew Marquardt [b], Norbert Kučerka [c,d,e], Thad A. Harroun [b], Maikel C. Rheinstädter [a,c,*]

[a] Department of Physics and Astronomy, McMaster University, Hamilton, ON, Canada
[b] Department of Physics, Brock University, St. Catharines, ON, Canada
[c] Canadian Neutron Beam Centre, Chalk River, ON, Canada
[d] Department of Physical Chemistry of Drugs, Comenius University, Bratislava, Slovakia
[e] Frank Laboratory of Neutron Physics, Joint Institute for Nuclear Research, Dubna, Russia

ARTICLE INFO

Article history:
Received 21 August 2014
Received in revised form 18 November 2014
Accepted 19 November 2014
Available online 2 December 2014

Keywords:
Lipid membranes
Cholesterol
Aspirin
Cholesterol rafts
Aspirin–cholesterol interaction

ABSTRACT

Aspirin and other non-steroidal anti-inflammatory drugs have a high affinity for phospholipid membranes, altering their structure and biophysical properties. Aspirin has been shown to partition into the lipid head groups, thereby increasing membrane fluidity. Cholesterol is another well known mediator of membrane fluidity, in turn increasing membrane stiffness. As well, cholesterol is believed to distribute unevenly within lipid membranes leading to the formation of lipid rafts or plaques. In many studies, aspirin has increased positive outcomes for patients with high cholesterol. We are interested if these effects may be, at least partially, the result of a non-specific interaction between aspirin and cholesterol in lipid membranes.

We have studied the effect of aspirin on the organization of 1,2-dipalmitoyl-*sn*-*glycero*-3-phosphatidylcholine (DPPC) membranes containing cholesterol. Through Langmuir–Blodgett experiments we show that aspirin increases the area per lipid and decreases compressibility at 32.5 mol% cholesterol, leading to a significant increase of fluidity of the membranes. Differential scanning calorimetry provides evidence for the formation of metastable structures in the presence of aspirin. The molecular organization of lipids, cholesterol and aspirin was studied using neutron diffraction. While the formation of rafts has been reported in binary DPPC/cholesterol membranes, aspirin was found to locally disrupt membrane organization and lead to the frustration of raft formation. Our results suggest that aspirin is able to directly oppose the formation of cholesterol structures through non-specific interactions with lipid membranes.

1. Introduction

Lateral heterogeneity in lipid composition in membranes permits the existence of so-called lipid rafts: regions of the membrane believed to contain elevated cholesterol composition and increased molecular order [1–4]. Domains serve a functional purpose as they are thought to take part in membrane-associated events such as lipid/protein sorting and signal transduction, among other roles [5–10]. Experimental observation of rafts has been challenging as they are believed to be both small and short lived [11–14].

Cholesterol is suggested to drive domain formation through lipid interactions with cholesterol's stiff ring structure leading to the so-called liquid ordered (l_o) phase [15–18]. Small, transient cholesterol domains in binary lipid bilayers at physiological levels of cholesterol were recently reported from computer simulations and experiments [18–23]. At high concentrations of cholesterol, above ~40 mol%, immiscible cholesterol bilayers were reported to form spontaneously in model lipid bilayers [24–28].

There is growing evidence for an influence of various pharmaceuticals on lipid membrane organization and stability [29]. In particular, non-steroidal anti-inflammatory drugs (NSAID's) have been shown to disturb bilayer structures in real and model membranes [30,31]. Aspirin (acetylsalicylic acid, ASA) is the most common NSAID and has been shown to have strong interactions with bilayer structures [30,32]. Aspirin strongly perturbs model membrane structures in a concentration dependent manner and influences human erythrocyte shape [33]. As well, aspirin decreases the hydrophobic surface barrier in mucosal membranes, leading to a diffusion of acid and gastrointestinal injury [34] and has an effect on protein sorting [35]. Recently, a direct interaction between aspirin and cholesterol was reported as aspirin was observed to reduce the volume of cholesterol plaques in model membranes with elevated cholesterol concentrations of 40 mol% [36].

Abbreviations: DPPC, dipalmitolyphosphatidylcholine; ASA, acetylsalicylic acid; DSC, differential scanning calorimetry; L-B, Langmuir–Blodgett; PG, pyrolytic graphite; TFE, trifluoroethanol; RH, relative humidity; COX, cyclooxygenase

* Corresponding author at: Department of Physics and Astronomy, McMaster University, ABB-241, 1280 Main Street West, Hamilton, Ontario L8S 4M1, Canada. Tel.: +1 905 525 9140 23134; fax: +1 905 546 1252.
E-mail address: rheinstadter@mcmaster.ca (M.C. Rheinstädter).

http://dx.doi.org/10.1016/j.bbamem.2014.11.023
0005-2736/

However, an influence of aspirin on membranes with physiological levels of cholesterol has not been explored.

We examined the effect of aspirin on membranes composed of DPPC and physiological levels of cholesterol. The molecules are depicted in Fig. 1. By combining Langmuir–Blodgett isotherms, calorimetric measurements and neutron diffraction, we present evidence that the presence of 10 mol% ASA leads to a significant re-fluidification of DPPC/32.5 mol% cholesterol bilayers. The neutron diffraction patterns are indicative of ASA super-structures in the fluid bilayers, which seem to frustrate the formation of cholesterol rafts.

2. Results

2.1. Langmuir–Blodgett monolayer compression isotherms

Pressure versus area isotherms were recorded for DPPC monolayers with and without cholesterol in order to determine molecular areas and compressibility. ASA was dissolved in the aqueous sub-phase at concentrations of 0 mM and 3 mM. All experiments were performed with a sub-phase temperature of 50 °C. Fig. 2a) shows the compression isotherms for all experiments. The addition of 32.5 mol% cholesterol to the monolayer shifts the isotherm towards lower pressures and lower area per lipid compared to a monolayer composed of pure DPPC. However, with the addition of 3 mM ASA into the water sub-phase, the compression isotherm shifted to higher pressures and higher area per lipid, for both pure DPPC monolayers and monolayers containing 32.5 mol% cholesterol. To best capture trends observed in the compression isotherms, a pressure of 27 mN/m was chosen to compare the changes in the monolayer area per molecule as well as in the compressibility modulus due to the incorporation of cholesterol and ASA.

The mean molecular area for all isotherms at a pressure of 27 mN/m is plotted in Fig. 2b). At this pressure, a DPPC monolayer has a mean area of $A_L = 71.9 \pm 0.5$ Å^2. The addition of 32.5 mol% cholesterol to the DPPC monolayers decreases A_L significantly to 38.6 ± 0.2 Å^2. Inclusion of 3 mM ASA in the sub-phase leads to an increase of the area per lipid to 74.4 ± 0.7 Å^2. The same effect is observed in the presence of cholesterol: the addition of 3 mM ASA in the sub phase leads to a significant increase of the area per lipid in DPPC/32.5 mol% cholesterol from 38.6 ± 0.2 Å^2 to 44.3 ± 0.3 Å^2.

The compressibility of the monolayers is determined by the slope of the isotherms (as detailed in the Materials and methods section, Section 4). The addition of ASA to the water sub-phase decreases the elastic compressibility modulus, C_S^{-1}, from 84 ± 1 mN/M for pure DPPC to 63 ± 1 mN/M for DPPC/3 mM ASA as depicted in Fig. 2c), at a pressure of 27 mN/m. This is in strong contrast to cholesterol, which increases the compressibility modulus when added to the monolayer from 84 ± 1 mN/M to 89.8 ± 0.3 mN/M, as reported previously [37,38]. Addition of ASA to the DPPC/32.5 mol% cholesterol monolayers reduces the compressibility from 89.8 ± 0.3 mN/M to 80.6 ± 0.5 mN/M.

A decreased compressibility modulus is indicative of membranes, which are softer and more compressible. The increase in molecular area and decrease in compressibility for a pure DPPC bilayer in the presence of aspirin points to a general increase in fluidity of the membranes. The increase in molecular area and decrease in compressibility for DPPC/32.5 mol% cholesterol bilayers is strong evidence for a re-fluidification of the bilayers at a physiological cholesterol concentration with ASA.

2.2. Differential scanning calorimetry

The effect of ASA on the phase behavior of membranes was examined using differential scanning calorimetry. Multi-lamellar vesicles (MLVs) of different composition were prepared for these experiments. Heating thermograms are plotted in Fig. 3a). A thermogram taken from a pure DPPC sample shows two endothermic transitions. There is a pre-transition from the gel to ripple phase ($L_\beta \rightarrow P_{\beta'}$) at T ~ 308 K. The main transition to the fluid phase (L_α) occurs at 314 K, in agreement with literature values [39]. Addition of ASA resulted in a decrease in the main transition temperature and broadened the main transition peak (and eliminated the pre-transition). Similar results have been reported when ASA is added to DMPC liposomes [33]. A reduction or suppression in transition temperatures and transition enthalpy is evidence that ASA reduces the cooperativity of the main and pre-transitions, indicative of a more fluid structure.

As expected, thermograms of samples composed of DPPC with 32.5 mol% cholesterol in Fig. 3b) show no transitions, as was reported previously for the l_o phase [20,40]. The absence of a transition proves that a cholesterol concentration of 32.5 mol% is high enough to induce the l_o phase in DPPC bilayers. No change was observed after addition of 1 mM ASA (data not shown). However, as shown in Fig. 3b), addition of 6 mM ASA led to the appearance of an exothermic transition at $T = 313.6$ K.

The bilayers were then cooled and the heating thermogram was repeated. After this second cycling the transition peak shifted to $T = 308$ K and significantly broadened. The temperature cycling was repeated, and a third thermogram shows no transition peak. We note that no peak was observed upon cooling, regardless of cycle number. The dependence of the thermogram upon temperature cycling indicates the presence of inhomogeneities and kinetically trapped states existing on

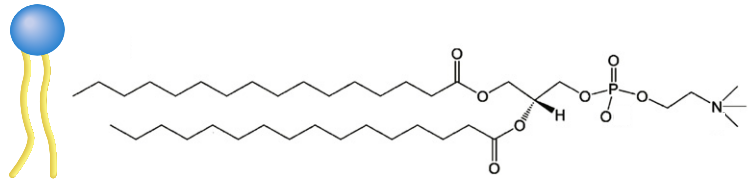

1,2-dipalmitoyl-sn-glycero-3-phosphatidylcholine (DPPC)

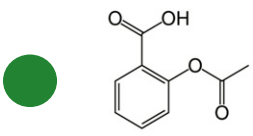

Acetylsalicyclic acid (ASA)

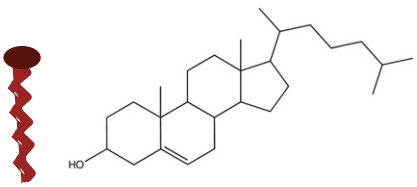

Cholesterol

Fig. 1. Schematic representations of the 1,2-dipalmitoyl-*sn-glycero*-3-phosphatidylcholine (DPPC), cholesterol, and acetylsalicylic acid (ASA, aspirin) molecules used in this study.

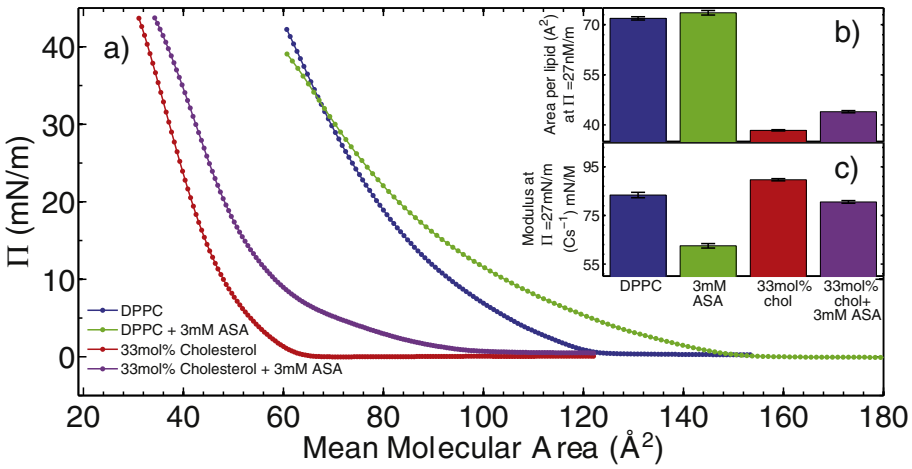

Fig. 2. Langmuir–Blodgett experiments were performed on DPPC monolayers with and without cholesterol. a) Compression isotherms of monolayers of DPPC (blue), DPPC with 3 mM ASA in the subphase (green), DPPC/32.5 mol% cholesterol (red) and DPPC/32.5 mol% cholesterol and 3 mM ASA in the subphase (purple). b) Area per lipid molecule for isotherms at $\Pi = 27$ mN/m for all samples. c) Compressibility modulus (C_S^{-1}) for all samples, measured at $\Pi = 27$ mN/m.

timescales comparable to the rate of cycling [41–43]. The caloric data point, therefore, to the existence of meta-stable structures in cholesterol bilayers in the presence of ASA, as will be discussed below.

2.3. Neutron diffraction

Lateral molecular order of chain perdeuterated DPPC bilayers containing 32.5 mol% cholesterol and 10 mol% ASA was studied using in-plane neutron diffraction. Rafts have been reported at this concentration of cholesterol in DPPC bilayers from computer simulations and experiments [18–23]. Highly oriented, solid supported membranes were prepared and placed in a humidity chamber at $T = 50$ °C and a D_2O relative humidity of ~100%, ensuring full hydration of bilayers. Bilayers made of DPPC/32.5 mol% cholesterol were previously studied using this setup by Armstrong et al. [20] and d_z-spacings of 64 Å were observed, in good agreement with lamellar spacings reported by Gallová et al. [53] in multi-lamellar DPPC liposomes with 33.3 mol% cholesterol. This proves that fully hydrated bilayers can be prepared using our technique.

Two different neutron scattering setups were used: (1) a conventional high energy and momentum resolution setup and (2) a low energy and momentum resolution setup, which permits greater spatial resolution for detecting small structures and weak signals, as reported previously [20,23,44,45]. The two setups were achieved by changing the incoming neutron wavelength, λ, without any need to re-align the sample or change the hydration state of the bilayers. By using chain perdeuterated DPPC-d62, our experiment was predominantly sensitive to molecular structure and arrangement of the lipid acyl chains. The sample was aligned in the neutron beam such that the scattering vector, $\vec{Q}$, was always in the plane of the membranes. This in-plane component of the scattering vector is referred to as $q_{||}$.

Data taken using the conventional setup is shown in Fig. 4a). Sharp peaks occur at $q_{||} = 1.1$ Å^{-1} and 1.65 Å^{-1}, which are assigned to scattering from silicon (in higher orders) and are highlighted in gray. The

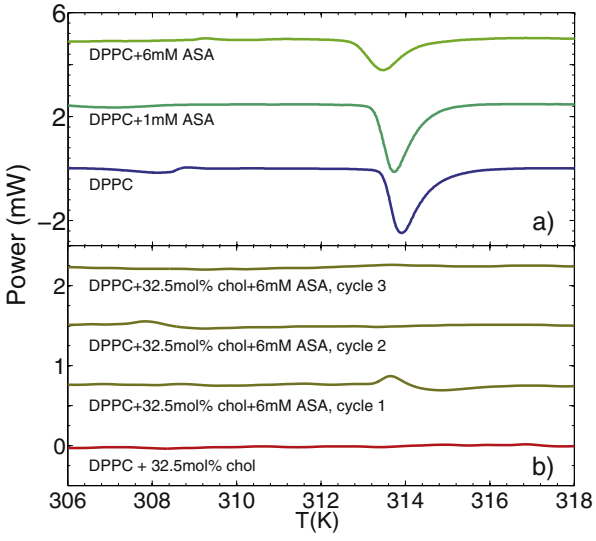

Fig. 3. Differential scanning calorimetry studies of multi-lamellar vesicles with cholesterol and ASA. a) Heating scans of pure DPPC membranes with different ASA concentrations in the aqueous phase. b) Heating scans of DPPC membranes with 32.5 mol% cholesterol. With no ASA in the sub-phase, a heating scan shows no feature indicating membranes with 32.5 mol% cholesterol are in the l_o phase. However, addition of 6 mM ASA leads to the appearance of an additional feature, which is unstable upon repeated heating scans.

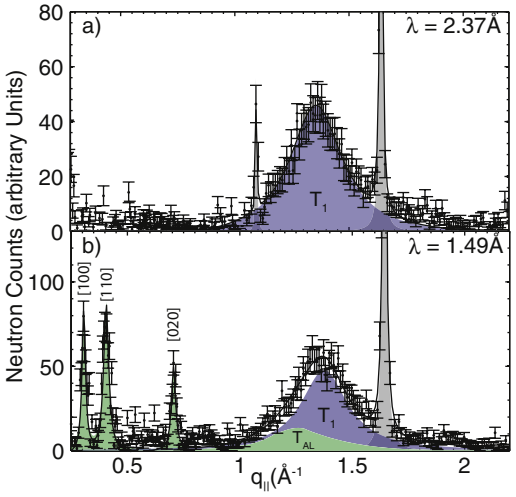

Fig. 4. In-plane neutron diffraction profiles of DPPC-d62 membranes containing 32.5 mol% cholesterol and 10 mol% ASA. a) An in-plane profile recorded with a typical low spatial resolution setup. The sharp gray peaks at $q_{||} = 1.1$ Å^{-1} and 1.65 Å^{-1} originate, respectively, from 3rd and 2nd order scattering of silicon. The single feature, typically observed in diffraction patterns, is a broad correlation peak due to the packing of the lipid tails in the hydrophobic membrane core. b) An in-plane profile recorded with a high spatial resolution setup. Additional, narrow and pronounced features appear with change in resolution, as explained in the text.

diffraction pattern shows a single broad peak centered at $q_{||} \sim 1.36$ Å^{-1}, indicated in blue. The broad correlation peak was well described by a Lorentzian peak profile, and was previously assigned to a hexagonal packing of the lipid acyl chains in the hydrophobic membrane core with parameters $a_{lipid-l_o} = b_{lipid-l_o} = 5.58$ Å and $\gamma = 120°$ [20,23]. The data in Fig. 4a) show a diffraction pattern typical of a fluid, liquid-ordered (l_o) membrane.

The diffraction pattern obtained using a high spatial resolution is shown in Fig. 4b). In addition to a broad correlation peak and sharp peaks originating from silicon, three narrow and pronounced correlation peaks are visible, indicating a coexisting and well-ordered lateral structure. The broad correlation peak at $q_{||} \sim 1.36$ Å^{-1} is no longer well described by a single distribution. Rather, two Lorentzian profiles were required to fit the observed scattering: (1) a peak located at $q_{||} \sim 1.37$ Å^{-1} (in agreement with part a)); and (2) a weaker peak at $q_{||} \sim 1.28$ Å^{-1}. The latter is highlighted by the green profile in Fig. 4b). The observation of two peak profiles suggests the presence of two environments for the lipid tails in the presence of ASA. The integrated area of the green Lorentzian at smaller $q_{||}$-values in Fig. 4b) is ~1/3 the integrated area of the blue profile. The concentration of ASA and DPPC in the bilayers is 10 mol% and 60.75 mol% respectively, resulting in a ratio between ASA and lipid molecules of ~1/6. The ratio between the integrated intensities is then indicative that one ASA molecule interacts with two lipid molecules leading to a lipid environment with a larger tail spacing.

The position of the sharp peaks ($q_{||} = 0.305$ Å^{-1}, $q_{||} = 0.41$ Å^{-1}, $q_{||} = 0.705$ Å^{-1}) are best indexed by the [100], [110] and [020] reflections, respectively, of a monoclinic unit cell with parameters $a_{superlattice} = 21.2$ Å, $b_{superlattice} = 18.2$ Å, $\gamma = 104°$. The dimensions of the unit cell suggest the formation of a super-lattice-type structure, containing several lipid and cholesterol molecules. The corresponding molecular structure is depicted in Fig. 5. We note that the diffraction pattern in Fig. 4b) does not show evidence for the highly ordered, monoclinic lipid raft structure, which was observed previously by Armstrong et al. in DPPC/32.5 mol% cholesterol bilayers through neutron diffraction.

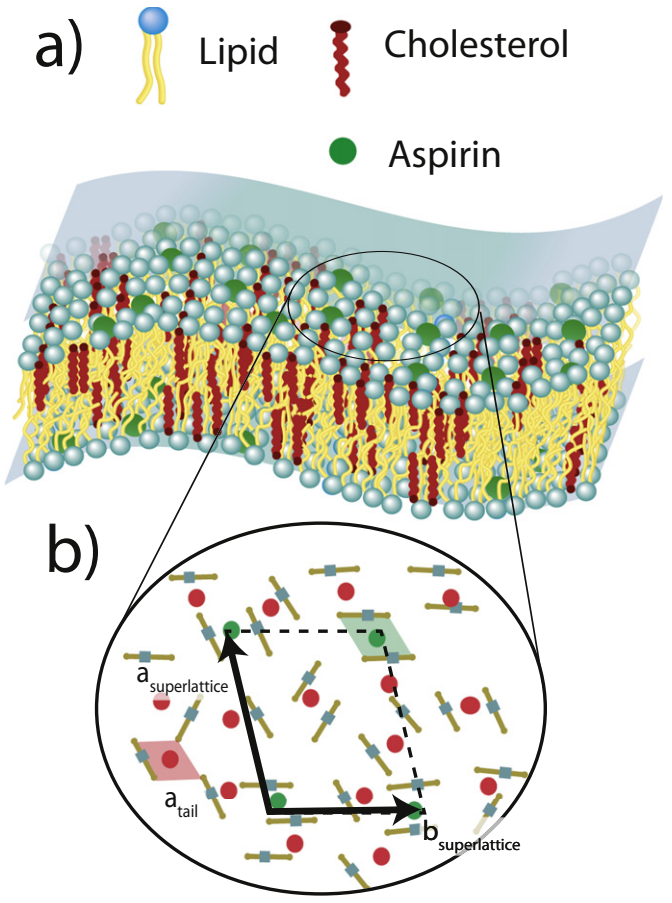

Fig. 5. Cartoon of a DPPC membrane containing 32.5 mol% cholesterol and 10 mol% ASA, as deduced from the neutron diffraction data in Fig. 4a). A depiction of a bilayer containing cholesterol and ASA. b) A cartoon of the super-lattice as imaged by the high spatial resolution setup. The black arrows highlight a super-lattice cell, determined from the diffraction pattern in Fig. 4b). The different lipid environments are highlighted by the green and red parallelograms.

3. Discussion and conclusions

When introduced into the body, aspirin and its metabolites are understood to interact through specific biochemical reactions. Aspirin is known to interact with the cyclo-oxygenase (COX) pathway. The inhibition of both COX isoforms, COX-1 and COX-2, by higher dose aspirin is believed to lead to analgesic and anti-inflammatory effects, while lower doses, sufficient to inhibit COX-1 activity, leads to anti-platelet activity [46,47]. However, there is evidence for the role of platelet membrane composition and fluidity in determining platelet cell function [48–50]. Platelet aggregation has also been associated with lipid rafts [51]. As discussed in the Introduction, there is growing evidence for an interaction of aspirin with lipid membranes through non-specific effects.

As a prerequisite for such non-specific interactions, aspirin was reported to partition into lipid bilayers and position itself in the lipid head group region [32,36]. Our experiments suggest that aspirin is able to directly interact with model lipid membranes and oppose the molecular level organization induced by cholesterol.

We studied the interaction between DPPC bilayers containing 32.5 mol% cholesterol and ASA using three different techniques, namely Langmuir–Blodgett experiments, differential scanning calorimetry and neutron diffraction. At this physiological cholesterol concentration, the DPPC bilayers are in their liquid-ordered phase. The l_o phase in binary DPPC/cholesterol bilayers was recently reported to form rafts [18–23] from experiments and simulations.

In order to use the different experimental techniques, different systems were prepared: monolayers were used in the Langmuir–Blodgett experiments, fully hydrated multilamellar vesicles in the calorimetric experiments and highly oriented solid supported multilamellar bilayers hydrated through the vapor phase in the neutron diffraction experiments. We note that the area per molecule in the lipid monolayers of ~72 Å^2 is larger than the area per lipid reported for multilamellar DPPC bilayers of ~64 Å^2 [52]. The lamellar spacing that we determine at ~57 Å is significantly lower than the d_z-spacing of ~65 Å reported for fully DPPC/32.5 mol% cholesterol bilayers [20,53]. While we attribute the reduction in d_z-spacing mainly to the presence of ASA in the bilayers, we cannot exclude that the bilayers in our study did not achieve full hydration, as no reference values are published in the literature. Nevertheless, qualitatively similar results were observed when ASA was added to each of the systems: the bilayers showed an increase in fluidity and the effects of cholesterol are countered. We, therefore, can argue that the conclusions we draw below are robust and supported by the experiments.

10 mol% ASA was added to the membranes, i.e., 1 ASA molecule per 10 lipid molecules. This ASA concentration is elevated as compared to plasma concentrations of less than 1 mol%, however, comparable to ASA concentrations typically used in the literature [54]. Floating monolayers were used to determine the area per molecule and compressibility in the presence of ASA. Multi-lamellar vesicles were studied in the calorimetric experiments to determine the effect of ASA on the phase behavior. Finally, solid supported bilayers were used for neutron diffraction experiments to study arrangement of the molecules in the plane of the membranes.

Several conclusions can be drawn from this combination of techniques and systems. ASA interacts with monolayers, vesicles and

supported bilayers, independent of whether membranes were formed first and ASA was added to the aqueous phase (monolayers and vesicles) or included in the membranes at the time of the bilayer formation (solid supported bilayers). From the trough experiments, ASA leads to an increase in the area per molecule and a decrease in compressibility in pure DPPC and in DPPC/32.5 mol% cholesterol systems, indicative of a significant fluidification of the membranes. We note that ASA was reported previously by Alsop et al. [36] to dissolve cholesterol plaques, which form at higher cholesterol concentrations above ~40 mol%.

This increase in fluidity is also seen as a loss of cooperativity in the calorimetric experiments as broadening of the endothermic main transition in DPPC bilayers [41]. As a fingerprint of the l_o-phase, the main transition is suppressed in DPPC/32.5 mol% cholesterol bilayers. However, addition of 6 mM ASA to the aqueous phase led to the formation of a meta-stable phase in DPPC/cholesterol bilayers, as evidenced by an exothermic peak in the thermogram upon heating, which was shifted and eventually disappeared upon temperature cycling. Similar results were found when a quinoline antibiotic was studied with DPPC membranes [55], and it was suggested that the inclusion interaction of the drug with membranes led to the formation of meta-stable structures in the bilayers. Similar behavior can be observed in orientational glasses caused by a dynamic domain pattern and often related to aging and memory effects [56,57].

Neutron diffraction of oriented bilayers, using deuterium labeled lipid molecules, was used to study potential lateral structures in the presence of aspirin. Neutron measurements were taken at a constant temperature of 323 K, as continuous temperature cycling was not possible given the long counting times required for data collection. At low spatial resolution, the in-plane neutron diffraction pattern is indicative of a membrane in a uniform, disordered fluid state as reported previously [20,58,59]. The broad correlation peak in Fig. 4a) is the result of the hexagonal packing of the lipid acyl chains in the hydrophobic membrane core (planar group p6), as reported from, e.g., neutron diffraction [20].

With an increase in spatial resolution the lipid correlation peak is best described by two Lorentzian peak profiles, suggestive of two short-ranged lipid correlations and corresponding environments. A small, broad peak at $q_{||} \sim 1.28$ Å^{-1}, equivalent of an increased tail spacing, is associated with lipids interacting with aspirin molecules. The additional narrow and pronounced monoclinic super-lattice peaks are also driven by the presence of aspirin in the membrane. The corresponding molecular structure is depicted in Fig. 5. The ASA molecules, and the interacting lipid molecules, organize in a regular pattern throughout the membrane. Based on the ratio between the lipid chain peaks in the neutron data, each ASA molecule associates with two lipid molecules. This structure was observed with a neutron setup, which measured $q_{||}$ with $q_z = 0$. We can, therefore, not comment on whether the observed in-plane superlattice is possibly correlated across bilayers in the membrane stack.

This structure is different from the structure typically observed in binary DPPC/cholesterol membranes. While rafts were reported from computer simulations [19,21,22] and experiments [20,23], the presence of the ASA molecules in the bilayers seems to frustrate the formation of locally ordered cholesterol domains. While correlation peaks corresponding to raft structures were reported from neutron diffraction by Armstrong et al. [20] and Toppozini et al. [23] in DPPC/32.5 mol% cholesterol, these peaks were not observed in the diffraction data in Fig. 4, indicative that raft formation is inhibited in the presence of ASA.

In summary, the effect of aspirin (acetylsalicylic acid, ASA) on the structure of fluid lipid membranes made of DPPC containing 32.5 mol% cholesterol was studied at a concentration of 10 mol% ASA. Langmuir–Blodgett experiments suggest that ASA interacts with DPPC monolayers from the aqueous phase and leads to a fluidification of DPPC and DPPC/cholesterol membranes. Signatures of meta-stable patterns were observed in differential scanning calorimetry experiments. The corresponding molecular structure was determined from neutron diffraction. The observed diffraction pattern indicates that the presence of ASA leads to the formation of a super-lattice and the frustration of highly ordered cholesterol domains that were reported in binary DPPC/cholesterol membranes previously.

Although an interaction between aspirin and cholesterol was studied using three different membrane systems, the results in all systems suggest that ASA is able to counteract the effects of cholesterol when interacting with fluid lipid membranes. ASA induces changes to both the domain structure and the mechanical properties of DPPC membranes. These results add to the growing evidence for the potential of ASA to have a profound influence on the properties of membranes through non-specific interactions.

4. Materials and methods

Lipids and cholesterol were purchased from Avanti Polar Lipids (Alabaster, AL) and used without further purification. Acetylsalicylic acid (>99% crystalline) was purchased from Sigma Aldrich (Mississauga, ON).

4.1. Preparation of Langmuir monolayers and measurement of isotherms

Langmuir isotherms were performed on a KSV NIMA Minitrough (50 mm × 155 mm) and delrin barriers. Barrier control and data acquisition were achieved using the LB measurement system provided by KSV NIMA (Biolin Scientific, Linthicum Heights, Maryland USA). The balance was calibrated using a 264.9 mg calibration standard provided by the manufacturer prior to the commencement of the experiments.

Surface pressures were measured using pre-wetted paper Wilhemy plates at temperatures of 50 °C. Ultrapure (18.2 MΩ cm) water performed the role of the sub-phase. The sub-phase pressure was kept below 0.1 mN/m prior to spreading the lipid. If the pressure exceeded 0.1 mN/m, the surface was re-cleaned and the procedure repeated. Phospolipid films were spread by careful deposition of 2 μL volumes of chloroform solution containing 3 mg/mL lipid solution. After deposition, 10 min was allotted for solvent evaporation. The compression rate was 5 cm^2/min. Two lipid solutions were prepared: a pure DPPC solution, and a solution composed of DPPC/32.5 mol% cholesterol, both with concentrations at 3 mg/mL. Sub-phase solutions with two different concentrations of ASA were prepared: 0 mM ASA and 3 mM ASA.

The elastic compressibility can be determined from the pressure versus area isotherm, by calculating the corresponding slope:

$$C_s^{-1} = -A\left(\frac{d\pi}{dA}\right), \tag{1}$$

with $C_S{}^{-1}$ being the compression modulus, A the area in the trough and π the pressure.

4.2. Differential scanning calorimetry

Solutions of DPPC and DPPC with 32.5 mol% cholesterol were prepared in chloroform, then dried. Mixtures were placed under vacuum for ~6 h to ensure that all residual solvent was removed. Samples were then hydrated with ultrapure water (18.2 MΩ cm), with ASA concentrations of 0 mM, 1 mM and 6 mM to final DPPC concentrations of 125 mg/mL. Samples were put through 5 freeze/thaw cycles with vortexing, ensuring during the thaw step the solutions reached 50 °C. 25 μL of solution was loaded into Shimadzu Aluminum Hermetic Pans and crimp sealed. Thermograms were collected at 1 °C/min and a sampling rate of 1 s using a Shimadzu DSC-60 and a TA-60WS Thermal Analyzer.

4.3. Supported bilayer preparation

Highly oriented bilayers of 1,2-dipalmitoyl-sn-glycero-3-phosocholine (DPPC) containing cholesterol and acetylsalicylic acid

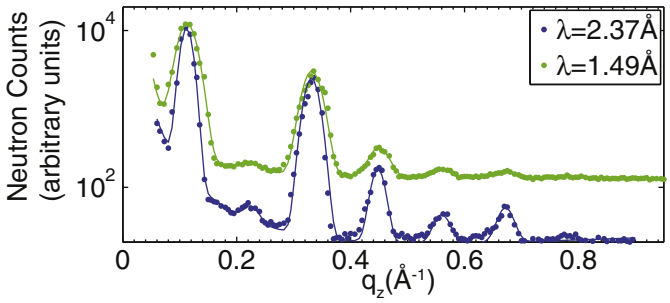

Fig. 6. Neutron reflectivities measured simultaneously with the in-plane data. Results from the typical setup are shown in blue, and results from the high spatial resolution setup are shown in green. The reflectivity shows a series of equally spaced and pronounced reflections, indicative of a well-ordered multi-lamellar membrane structure.

(ASA) were prepared by lipid deposition onto silicon wafers. The coherent scattering of lipid hydrocarbon chains was enhanced using chain perdeuterated lipids, DPPC-d62. A solution of 16.67 mg/mL of DPPC-d62 with 32.5 mol% cholesterol and 10 mol% ASA in 1:1 chloroform and 2,2,2-trifluoroethanol was prepared. 2 inch circular silicon wafers with a thickness of ~300 μm were cleaned with 12 min alternate sonications in methanol and ultrapure water (18.2 MΩ cm) at 310 K. This process was repeated twice. Clean, dry wafers were individually placed on a 4 in. × 4 in. marble block. The marble block was heated to 323 K, well above the main transition temperature of DPPC, ensuring that lipids were well in the fluid state during deposition. 1.2 mL of the lipid solution was deposited on the silicon wafer. Immediately after deposition, the marble block was manually lifted and gently rocked while the bulk of the solution evaporated (~1–2 min), to ensure even coverage of material.

The wafers were kept under vacuum overnight at 310 K to remove all traces of solvent. Nineteen such wafers were then stacked with 0.6 mm alumium spacers placed in between each wafer, to ensure proper hydration control. This "sandwich" sample was then placed inside a sealed container with a beaker of heavy water and placed in an incubator. The temperature of the incubator was increased in discrete steps from 300 K to 323 K over a period of 24 h, then held at 323 K and incubated for additional 24 h. Following this procedure, each wafer contained ~3000 highly oriented stacked membranes with a total thickness of ~10 μm.

During the neutron experiment, the sample was sealed in a temperature controlled aluminium chamber (CNBC, Chalk River, Canada). Hydration of the membranes from the vapor phase was achieved by separately controlling the temperature of a heavy water bath, the sample, and the walls of the chamber. Temperature sensors were installed close to the sample. A circulating water bath was used to control the temperature of the reservoirs and peltier elements were used to control the temperature of the sample and chamber. The sample was mounted vertically in the neutron beam such that the scattering vector, $\vec{Q}$, could either be placed in the plane of the membrane ($q_{||}$) or perpendicular to it (q_z). The out-of-plane and in-plane structures could be measured simply by rotating the sample by 90°.

Table 1
Peak parameters of the correlation peaks observed in Fig. 4a) and b) and the association with the observed structures, such as the l_o phase, lipids associated with ASA molecules and the super-lattice driven by the presence of ASA molecules. T_1 denotes the unit cell of the lipid tails in the l_o regions of the membrane. T_{AL} denotes the peak assigned to correlations between lipid molecules when influenced by ASA. Peaks were fitted using Lorentzian peak profiles and the corresponding widths are listed as Lorentzian widths (HWHM), γ_L.

	Amplitude (counts)	Center (Å^{-1})	γ_L (Å^{-1})	l_o	ASA bound lipids	Super-lattice phase
Fig. 4a)	48	1.36	0.14	T_1		
Fig. 4b)	85	0.306	0.01			[1 0 0]
	89	0.406	0.014			[1 1 0]
	50	0.705	0.011			[0 2 0]
	14	1.26	0.14		T_{AL}	

Table 2
Instrumental parameters of the triple-axis spectrometer.

λ (Å)	E (meV)	ΔE (meV)	ΔQ (Å^{-1})
2.37	14.6	0.757	0.020
1.49	37.3	3.239	0.032

The lamellar spacing, i.e., the distance between membranes in the stack, d_z, was determined from reflectivity scans. The corresponding out-of-plane or reflectivity scans are shown in Fig. 6, and show a series of pronounced and evenly spaced Bragg peaks indicative of uniform and well developed membrane stacks. Scans were performed with different wavelengths and over the duration of the experiment of two weeks. During the experiment, the bilayer spacing stayed within the range 55.8 Å and 57.9 Å. This setup has been used before to produce fluid DPPC bilayers [20,44] with d_z-spacings in agreement with literature values for fully hydrated bilayers of ~64 Å [20,58]. The observed decrease in lamellar spacing is most likely the effect of the incorporation of ASA in the bilayers, in agreement with the increased fluidification found in the trough and calorimetric experiments. The main transition of DPPC-d62 is reported as 313 K [60,61]. All scans were done with a sample temperature of 323 K, well above the main transition, in the fluid phase of the bilayers.

4.4. Neutron experiment

Experiments were conducted using the N5 triple axis spectrometer at the Canadian Neutron Beam Centre (Chalk River, Canada). The three axis of the spectrometer refer to the axis of rotation of the monochromator, the sample and the analyzer. The incident and final wavelengths were defined by Bragg reflections from pyrolytic graphite (PG) crystals. The divergence of the beam was controlled by Soller collimators. The energy and momentum (Q) resolution, ΔE and ΔQ, of a neutron triple axis spectrometer are determined by: (1) the incident energy of the neutron beam; (2) the divergence of the neutron beam; (3) the wavelength resolution of the monochromator and analyzer crystal. Collimation of the beam was held constant during the experiment and set to ($c1$-$c2$-$c3$-$c4$): 30-18-28-60 (in minutes). Small and large ΔE setups were achieved by varying the incident energy and corresponding neutron wavelength selected by the monochromator.

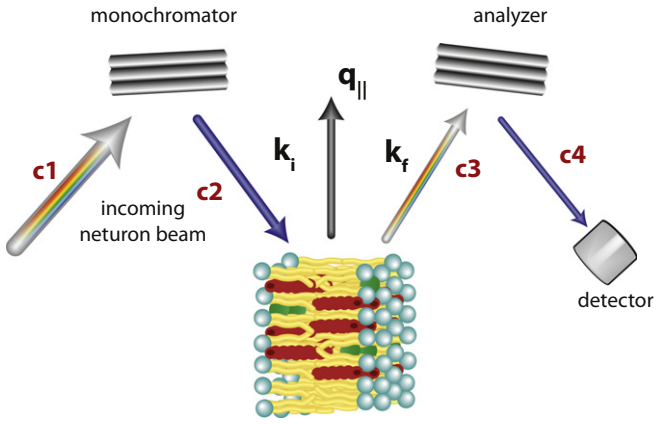

Fig. 7. A diagram of the setup used for the neutron scattering experiment. The orientation of the sample was chosen such that the scattering vector, $\vec{Q}$, lies in the plane of the membrane and is designated $q_{||}$. k_i and k_f are the incident and final neutron wave vectors. The c's indicate the collimation of the neutron beam at various stages. The resolution of the experiment is changed by rotating the monochromating crystal and selecting a different neutron wavelength.

The instrumental parameters for the two setups used in this experiment are listed in Table 2. Energy and Q-resolution (given as FWHM) were calculated using the ResLib software package by A. Zheludev [62] adapted to the N5 spectrometer. The longitudinal coherence length of the neutron beam, ξ, is defined by $\xi = \lambda^2/\Delta\lambda$.

While small collimation was used, the beam size was set to 2 in. by 2 in. to optimally illuminate the silicon wafers, leading to a significant scattering contribution at small Q-values, close to the direct beam. This background was accounted for by a Lorentzian peak centered at $q_{||} = 0\ \text{Å}^{-1}$ including a constant. In contrast to coherent scattering, incoherent scattering is isotropic, Q-independent and well accounted for by a constant background at larger Q-values of $Q \gtrsim 0.45\ \text{Å}^{-1}$. After background subtraction, the observed peaks were fit with Lorentzian profiles using a least squares method, and the results plotted in Fig. 4, with the fitting parameters presented in Table 1.

Switching between the high and low energy resolution setups was done by simply changing λ. A smaller neutron wavelength leads to strongly relaxed ΔQ and ΔE. In addition, the longitudinal coherence length of the neutron beam decreases. The most significant changes between the high and low energy resolution setups are: (1) a more efficient integration over larger $q_{||}$ ranges to enhance small signals; and (2) a reduction of the coherently added scattering volume. A diagram of the scattering geometry for the in-plane measurements is depicted in Fig. 7.

Acknowledgements

This research was funded by the Natural Sciences and Engineering Research Council (NSERC) of Canada, the National Research Council (NRC), the Canada Foundation for Innovation (CFI), and the Ontario Ministry of Economic Development and Innovation. R.J.A. is the recipient of an Ontario Graduate Scholarship, L.T. is the recipient of an NSERC Canada Graduate Scholarship, M.C.R. is the recipient of an Early Researcher Award from the Province of Ontario. D.M. is the recipient of an NSERC Vanier Canada Graduate Scholarship.

References

[1] K. Simons, E. Ikonen, Functional rafts in cell membranes, Nature 387 (1997) 569572.
[2] K. Simons, E. Ikonen, How cells handle cholesterol, Science 290 (2000) 1721–1726.
[3] D.M. Engelman, Membranes are more mosaic than fluid, Nature 438 (2005) 578–580.
[4] L.J. Pike, The challenge of lipid rafts, J. Lipid Res. 50 (2009) S323–S328.
[5] D. Lingwood, K. Simons, Lipid rafts as a membrane-organizing principle, Science 327 (2010) 46–50.
[6] C. Eggeling, C. Ringemann, R. Medda, G. Schwarzmann, K. Sandhoff, et al., Direct observation of the nanoscale dynamics of membrane lipids in a living cell, Nature 457 (2009) 1159–1162.
[7] F.G. van der Goot, T. Harder, Raft membrane domains: from a liquid-ordered membrane phase to a site of pathogen attack, Semin. Immunol. 13 (2001) 89–97.
[8] T. Apajalahti, P. Niemelä, P.N. Govindan, M.S. Miettinen, E. Salonen, et al., Concerted diffusion of lipids in raft-like membranes, Faraday Discuss. 144 (2010) 411–430.
[9] A. Hall, T. Róg, M. Karttunen, I. Vattulainen, Role of glycolipids in lipid rafts: a view through atomistic molecular dynamics simulations with galactosylceramide, J. Phys. Chem. B 114 (2010) 7797–7807.
[10] K. Simons, M.J. Gerl, Revitalizing membrane rafts: new tools and insights, Nat. Rev. Mol. Cell Biol. 11 (2010) 688–699.
[11] J. Ehrig, E.P. Petrov, P. Schwille, Phase separation and near-critical fluctuations in two-component lipid membranes: Monte Carlo simulations on experimentally relevant scales, New J. Phys. 13 (2011) 045019.
[12] T. Murtola, T. Róg, E. Falck, M. Karttunen, I. Vattulainen, Transient ordered domains in single-component phospholipid bilayers, Phys. Rev. Lett. 97 (2006) 238102.
[13] B. Brüning, E. Wald, W. Schrader, R. Behrends, U. Kaatze, Slowing down in lipid bilayers: domain structure fluctuations and axial diffusion, Soft Matter 5 (2009) 3340–3346.
[14] M.C. Rheinstädter, O.G. Mouritsen, Small-scale structure in fluid cholesterol-lipid bilayers, Curr. Opin. Colloid Interface Sci. 18 (2013) 440–447.
[15] J.H. Ipsen, O.G. Mouritsen, M.J. Zuckermann, Theory of thermal anomalies in the specific heat of lipid bilayers containing cholesterol, Biophys. J. 56 (1989) 661–667.
[16] M.R. Vist, J.H. Davis, Phase equilibria of cholesterol/dipalmitoylphosphatidylcholine mixtures: deuterium nuclear magnetic resonance and differential scanning calorimetry, Biochemistry 29 (1990) 451–464.
[17] C.L. Armstrong, M.A. Barrett, A. Hiess, T. Salditt, J. Katsaras, et al., Effect of cholesterol on the lateral nanoscale dynamics of fluid membranes, Eur. Biophys. J. 41 (2012) 901–913.
[18] C.L. Armstrong, W. Häußler, T. Seydel, J. Katsaras, M.C. Rheinstädter, Nanosecond lipid dynamics in membranes containing cholesterol, Soft Matter 10 (2014) 2600–2611.
[19] S. Meinhardt, R.L.C. Vink, F. Schmid, Monolayer curvature stabilizes nanoscale raft domains in mixed lipid bilayers, Proc. Natl. Acad. Sci. U. S. A. 110 (2013) 4476–4481.
[20] C.L. Armstrong, D. Marquardt, H. Dies, N. Kučerka, Z. Yamani, et al., The observation of highly ordered domains in membranes with cholesterol, PLoS ONE 8 (2013) e66162.
[21] A.J. Sodt, M.L. Sandar, K. Gawrisch, R.W. Pastor, E. Lyman, The molecular structure of the liquid-ordered phase of lipid bilayers, J. Am. Chem. Soc. 136 (2014) 725–732.
[22] Y. Zhang, A. Lervik, J. Seddon, F. Bresme, A coarse-grained molecular dynamics investigation of the phase behavior of dppc/cholesterol mixtures, Chem. Phys. Lipids (2014), http://dx.doi.org/10.1016/j.chemphyslip.2014.07.011.
[23] L. Toppozini, S. Meinhardt, C. Armstrong, Z. Yamani, N. Kučerka, et al., The structure of cholesterol in lipid rafts, Phys. Rev. Lett. 113 (2014) 228101.
[24] M. Barrett, S. Zheng, L. Toppozini, R. Alsop, H. Dies, et al., Solubility of cholesterol in lipid membranes and the formation of immiscible cholesterol plaques at high cholesterol concentrations, Soft Matter 9 (2013) 9342–9351.
[25] R. Ziblat, L. Leiserowitz, L. Addadi, Crystalline domain structure and cholesterol crystal nucleation in single hydrated DPPC:cholesterol:POPC bilayers, J. Am. Chem. Soc. 132 (2010) 9920–9927.
[26] R. Ziblat, L. Leiserowitz, L. Addadi, Crystalline lipid domains: characterization by X-ray diffraction and their relation to biology, Angew. Chem. Int. Ed. 50 (2011) 3620–3629.
[27] R. Ziblat, I. Fargion, L. Leiserowitz, L. Addadi, Spontaneous formation of two-dimensional and three-dimensional cholesterol crystals in single hydrated lipid bilayers, Biophys. J. 103 (2012) 255–264.
[28] I. Solomonov, J. Daillant, G. Fragneto, K. Kjaer, J. Micha, et al., Hydrated cholesterol: phospholipid domains probed by synchrotron radiation, Eur. Phys. J. A. 30 (2009) 215–221.
[29] M. Lucio, J. Lima, S. Reis, Drug-membrane interactions: significance for medicinal chemistry, Curr. Med. Chem. 17 (2010) 1795–1809.
[30] L.M. Lichtenberger, Y. Zhou, V. Jayaraman, J.R. Doyen, R.G. O'Neil, et al., Insight into nsaid-induced membrane alterations, pathogenesis and therapeutics: characterization of interaction of nsaids with phosphatidylcholine, Biochim. Biophys. Acta Mol. Cell Biol. Lipids 1821 (2012) 994–1002.
[31] C. Pereira-Leite, C. Nunes, S. Reis, Interaction of nonsteroidal anti-inflammatory drugs with membranes: *in vitro* assessment and relevance for their biological actions, Prog. Lipid Res. 52 (2013) 571–584.
[32] M. Barrett, S. Zheng, G. Roshankar, R. Alsop, R. Belanger, et al., Interaction of aspirin (acetylsalicylic acid) with lipid membranes, PLoS ONE 7 (2012) e34357.
[33] M. Suwalsky, J. Belmar, F. Villena, M.J. Gallardo, M. Jemiola-Rzeminska, et al., Acetylsalicylic acid (aspirin) and salicylic acid interaction with the human erythrocyte membrane bilayer induce *in vitro* changes in the morphology of erythrocytes, Arch. Biochem. Biophys. 539 (2013) 9–19.
[34] L.M. Lichtenberger, Y. Zhou, E.J. Dial, R.M. Raphael, Nsaid injury to the gastrointestinal tract: evidence that nsaids interact with phospholipids to weaken the hydrophobic surface barrier and induce the formation of unstable pores in membranes, J. Pharm. Pharmacol. 58 (2006) 1421–1428.
[35] Y. Zhou, K.J. Cho, S.J. Plowman, J.F. Hancock, Nonsteroidal anti-inflammatory drugs alter the spatiotemporal organization of ras proteins on the plasma membrane, J. Biol. Chem. 287 (2012) 16586–16595.
[36] R.J. Alsop, M.A. Barrett, S. Zheng, H. Dies, M.C. Rheinstädter, Acetylsalicylic acid (asa) increases the solubility of cholesterol when incorporated in lipid membranes, Soft Matter 10 (2014) 4275–4286.
[37] Y. Choi, S.J. Attwood, M.I. Hoopes, E. Drolle, M. Karttunen, et al., Melatonin directly interacts with cholesterol and alleviates cholesterol effects in dipalmitoylphosphatidylcholine monolayers, Soft Matter 10 (2014) 206–213.
[38] P. Wydro, K. Hac-Wydro, Thermodynamic description of the interactions between lipids in ternary Langmuir monolayers: the study of cholesterol distribution in membranes, J. Phys. Chem. B 111 (2007) 2495–2502.
[39] J. Katsaras, K.R. Jeffrey, Evidence of the hydration force in gel phase lipid multibilayers, Europhys. Lett. 38 (1997) 43–48.
[40] D. Marsh, Liquid-ordered phases induced by cholesterol: a compendium of binary phase diagrams, Biochim. Biophys. Acta Biomembr. 1798 (2010) 688–699.
[41] T. Heimburg, Thermal biophysics of membranes, John Wiley & Sons., 2008
[42] J. Jones, L. Lue, A. Saiani, G. Tiddy, Density, DSC, X-ray and NMR measurements through the gel and lamellar phase transitions of 1-myristoyl-2-stearoyl-sn-glycero-3-phosphatidylcholine (MSPC) and 1-stearoyl-2-myristoyl-sn-glycero-3-phosphatidylcholine (SMPC): observation of slow relaxation processes and mechanisms of phase transitions, Phys. Chem. Chem. Phys. 14 (2012) 5452–5469.
[43] A.M. Alaouie, A.I. Smirnov, Formation of a ripple phase in nanotubular dimyristoylphosphatidylcholine bilayers confined inside nanoporous aluminum oxide substrates observed by DSC, Langmuir 22 (2006) 5563–5565.
[44] C.L. Armstrong, M.A. Barrett, L. Toppozini, N. Kučerka, Z. Yamani, et al., Co-existence of gel and fluid domains in single-component phospholipid membranes, Soft Matter 8 (2012) 4687–4694.
[45] C.F. Majkrzak, C. Metting, B.B. Maranville, J.A. Dura, S. Satija, et al., Determination of the effective transverse coherence of the neutron wave packet as employed in reflectivity investigations of condensed-matter structures. I. Measurements, Phys. Rev. A 89 (2014) 033851.
[46] G.J. Roth, N. Stanford, P.W. Majerus, Acetylation of prostaglandin synthase by aspirin, Proc. Natl. Acad. Sci. U. S. A. 72 (1975) 3073–3076.

[47] C. Patrono, L.A. Garca Rodrguez, R. Landolfi, C. Baigent, Low-dose aspirin for the prevention of atherothrombosis, N. Engl. J. Med. 353 (2005) 2373–2383.
[48] V.B. O'Donnell, R.C. Murphy, S.P. Watson, Platelet lipidomics modern day perspective on lipid discovery and characterization in platelets, Circ. Res. 114 (2014) 1185–1203.
[49] S.J. Shattil, R.A. Cooper, Membrane microviscosity and human platelet function, Biochemistry (Mosc) 15 (1976) 4832–4837.
[50] P. Padmavathi, V.D. Reddy, P. Maturu, N. Varadacharyulu, Smoking-induced alterations in platelet membrane fluidity and na+/k+-ATPpase activity in chronic cigarette smokers, J. Atheroscler. Thromb. 17 (2010) 619–627.
[51] K. Gousset, W.F. Wolkers, N.M. Tsvetkova, A.E. Oliver, C.L. Field, et al., Evidence for a physiological role for membrane rafts in human platelets, J. Cell. Physiol. 190 (2002) 117–128.
[52] N. Kučerka, S. Tristram-Nagle, J.F. Nagle, Closer look at structure of fully hydrated fluid phase DPPC bilayers, Biophys. J. 90 (2006) L83–L85.
[53] J. Gallová, D. Uhrková, N. Kučerka, S. Doktorovová, S.S. Funari, et al., The effects of cholesterol and β-sitosterol on the structure of saturated diacylphosphatidylcholine bilayers, Eur. Biophys. J. 40 (2011) 153–163.
[54] M. Lúcio, C. Nunes, D. Gaspar, K. Golebska, M. Wisniewski, et al., Effect of anti-inflammatory drugs in phosphatidylcholine membranes: a fluorescence and calorimetric study, Chem. Phys. Lett. 471 (2009) 300–309.
[55] K. Nag, K. Keough, M. Montero, J. Trias, M. Pons, et al., Evidence of segregation of a quinolone antibiotic in dipalmitoylphosphatidylcholine environment, J. Liposome Res. 6 (1996) 713–736.
[56] A.V. Kityk, M.C. Rheinstädter, K. Knorr, H. Rieger, Aging and memory effects in β-hydroquinone-clathrate, Phys. Rev. B 65 (2002) 144415.
[57] M.C. Rheinstädter, K. Knorr, H. Rieger, Aging and scaling laws in β-hydroquinone-clathrate, Phys. Rev. B 69 (2004) 144427.
[58] T.T. Mills, G.E.S. Toombes, S. Tristram-Nagle, D.M. Smilgies, G.W. Feigenson, et al., Order parameters and areas in fluid-phase oriented lipid membranes using wide angle X-ray scattering, Biophys. J. 95 (2008) 669–681.
[59] M.C. Rheinstädter, C. Ollinger, G. Fragneto, T. Salditt, Collective dynamics in phospholipid bilayers investigated by inelastic neutron scattering: exploring the dynamics of biological membranes with neutrons, Physica B 350 (2004) 136–139.
[60] J. Katsaras, R. Epand, R. Epand, Absence of chiral domains in mixtures of dipalmitoylphosphatidylcholine molecules of opposite chirality, Phys. Rev. E. 55 (1997) 3751.
[61] S. Mabrey, J.M. Sturtevant, Investigation of phase transitions of lipids and lipid mixtures by sensitivity differential scanning calorimetry, Proc. Natl. Acad. Sci. 73 (1976) 3862–3866.
[62] A. Zheludev, Reslib, http://www.neutron.ethz.ch/research/resources/reslib 2009.